

Magnetoresistance oscillations and the half-flux-quantum state in spin-triplet superconductor Sr_2RuO_4

X. Cai,¹ Y. A. Ying,¹ J. E. Ortmann,² W.-F. Sun,² Z.-Q. Mao,² and Y. Liu^{1,3,4,*}

¹*Department of Physics and Materials Research Institute,*

Pennsylvania State University, University Park, PA 16802, USA

²*Department of Physics, Tulane University, New Orleans, LA 70118, USA*

³*Department of Physics and Astronomy, Shanghai Jiao Tong University,*

800 Dong Chuan Road, Shanghai 200240, China

⁴*Collaborative Innovation Center of Advanced Microstructures, Nanjing 210093, China*

(Dated: July 12, 2016)

We report results of our low-temperature magneto electric transport measurements on micron-sized short cylinders of odd-parity, spin-triplet superconductor Sr_2RuO_4 with the cylinder axis along the c axis. The in-plane magnetic field and measurement current dependent magnetoresistance oscillations were found to feature an amplitude much larger than that expected from the conventional Little-Parks effect, suggesting that the magnetoresistance oscillations originate from vortex crossing. The free-energy barrier that controls the vortex crossing was modulated by the magnetic flux enclosed in the cylinder, the in-plane field, measurement current, and structural factors. Distinct features on magnetoresistance peaks were found, which we argue to be related to the emergence of half-flux quantum states, but only in samples for which the vortex crossing is confined at specific parts of the sample.

PACS numbers:

Fluxoid quantization in a doubly connected conventional superconductor in the unit of a full flux-quantum, $\Phi_0 = hc/2e$ (where h is the Plank constant and e the electron charge), is a direct consequence of pairing of the electrons and the emergence of long-range phase coherence among the paired electrons.[1] Deaver and Fairbank[2] and Doll and N  bauer[3] measured the magnetic flux trapped in a superconducting hollow cylinder and the torque on the circulating supercurrent, respectively, to demonstrate this remarkable effect. The physics of this effect was further clarified by the Little and Parks (LP) experiment[4], demonstrating the oscillations in the superconducting transition temperature, T_c , and the periodic variation of the free energy with the applied magnetic flux in a doubly connected superconducting cylinder. Therefore, after the initial experimental evidence for the half-flux-quantum vortices[5] was found in the odd-parity, spin-triplet superconductor Sr_2RuO_4 [6–10] in the torque magnetometry experiment[11], the LP measurement has been highly desirable so as to obtain insights into the physics of the half-flux-quantum state in this unconventional superconductor.

The half-flux-quantum state is allowed in a spin-triplet superconductor along with the conventional full-flux-quantum state because of the presence of spin and orbital parts of the order parameter. A possible scenario is that a phase winding of π is formed separately in each part of the order parameter around a doubly connected sample or a vortex core to maintain the singlevaluedness of the order parameter. Only the circulating supercurrent due to the orbital phase winding features a magnetic flux, giving rise to a vortex state featuring a half-flux-quantum of $\Phi_0/2$. The free energy of the half-flux-quantum state

is usually higher than the conventional full-flux quantum one, making its physical realization difficult. For a doubly connected, micron-sized crystal of Sr_2RuO_4 , the free energy of the half-flux-quantum state appeared to be lowered near applied half-flux quanta by the application of an in-plane magnetic field[11] as proposed theoretically[12].

Recently we carried out magnetoresistance oscillation measurements on micron-sized, single crystal rings of Sr_2RuO_4 [13], in which a large number of pronounced resistance oscillations with an amplitude much larger than that expected from the LP effect were observed down to very low temperatures. The observed magnetoresistance oscillations were attributed to c -axis vortices moving across the sample that leads to a finite transverse voltage according to the Josephson relation[1]. The oscillation amplitude is controlled by the barrier potential for vortex crossing, which is a function of applied flux due to fluxoid quantization. No features associated with half-flux-quantum states were found over a wide range of the out-of-plane field without the application of an in-plane field. Interestingly, a fit of our data to the Ambegaokar-Halperin (AH) model of thermally activated vortex crossing over a free energy barrier[14, 15] yielded values of zero-temperature penetration depth much larger than that of the bulk[16], which is consistent with the small magnetic moments observed in the torque magnetometry experiment compared to the numerical calculation[17]. Here we present magnetoresistance oscillation measurements in the presence of an in-plane field with varying measurement currents and magnetoresistance signatures of the half-flux-quantum state, thereby providing insights into conditions favoring experimental observation of this

exotic state.

To prepare our samples, thin crystal plates of Sr_2RuO_4 were made on a Si/SiO_2 substrate by mechanical exfoliation from a bulk single crystal. Four- or six-point electrical leads, made of 200 nm Au and an underlay of 10 nm Ti, were prepared on the crystal plates by photolithography. A doubly connected cylinder with four leads was cut from the crystal plates using a focused ion beam (FIB), with Sr_2RuO_4 leads extending from the cylinder to the Ti/Au contacts. Fig. 1a shows a scanning electron microscopy (SEM) image of a typical cylinder, which has a height of about $0.74 \mu\text{m}$ and a wall thickness increasing from top to bottom due to the profile of the ion beam. This hollow cylinder has a mean wall-thickness (w) of $0.26 \mu\text{m}$ and a mean radius (r) of $0.58 \mu\text{m}$ as indicated in Fig. 1b. More details in sample fabrication and the estimation of sample dimensions can be found in reference [13]. Our samples were measured in a dilution refrigerator with a base temperature of 20 mK, using a dc technique. Since both the out-of- and the in-plane fields, $H_{\parallel c}$ and $H_{\parallel ab}$, are needed, a homemade superconducting Helmholtz coil was incorporated inside a large superconducting solenoid.

Almost all Sr_2RuO_4 samples prepared this way were found to be superconducting with an onset T_c sample dependent. In Fig. 1c, the temperature dependent resistance data revealed a broad transition with a zero-resistance T_c dependent on the measurement current. A resistance peak was found around 1.6 K, an anomaly observed previously in superconducting nanowires and attributed to charge imbalance encountered when superconducting voltage leads were used. [18] The onset T_c of these samples is higher than the bulk phase, 1.5 K, likely due to the presence of dislocations in the thin crystal plates of Sr_2RuO_4 . [19]

We measured the sample resistance as a function of the in-plane field, $H_{\parallel ab}$, aligned perpendicular to the current leads (Fig. 1b). Hysteresis as well as fluctuations were observed (Fig. 1d), especially for the curves measured at a low temperature, 0.6 K, possibly due to the depinning of parallel vortices. Even though the in-plane field could be misaligned from the ab -plane of the cylinders by a small angle, the vortices in the sample should still be aligned in the in-plane direction because of the strong anisotropy of Sr_2RuO_4 . The critical field, at which the sample resistance becomes non-zero, was found to decrease with the increasing measurement current. It should be noted that the c -axis vortices can appear simultaneously in Sr_2RuO_4 crystals. [20, 21]

Pronounced magnetoresistance oscillations were observed at fixed temperatures as the out-of-plane field, $H_{\parallel c}$, was ramped up (Fig. 2). The oscillation period is Φ_0 based on the sample dimensions. A large measurement current was used in order for the magnetoresistance oscillations to be measured at such low temperatures. The vortex crossing origin of the magnetoresistance oscilla-

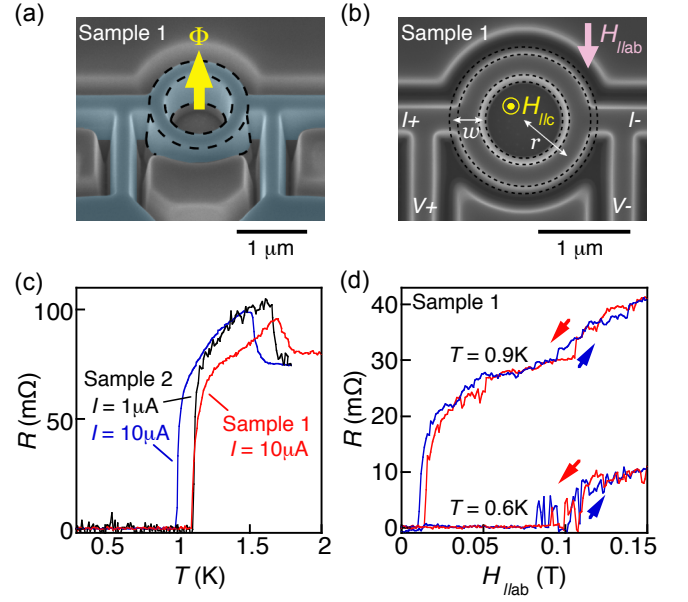


FIG. 1: (a) A false-color SEM image of Sample 1 prepared on a Si/SiO_2 substrate. The cylinder and the leads (in blue) were covered by a layer of SiO_2 used to protect the crystal during the FIB cutting. The image was taken at a 30° angle from the axial direction. The slightly increased wall thickness towards the bottom of the cylinder is evident. (b) A SEM image of the sample in (a) showing the measurement setup. The outer edges of the cylinder on the top and the bottom surfaces of the crystal plate are indicated. (c) Temperature dependence of sample resistance, R vs. T , measured for two samples with applied currents, I , as indicated. Sample 2 has the same w and r as Sample 1 and a height of about $0.78 \mu\text{m}$. (d) Sample resistance as the function of the in-plane field, R vs. $H_{\parallel ab}$, at two different temperatures with $I = 30 \mu\text{A}$. Arrows indicate the field sweeping directions.

tions is confirmed by a quantitative comparison between the experimental values of the oscillation amplitude and that expected from the conventional LP effect. No obvious feature corresponding to the transition between half- and full-flux quantum states in the resistance oscillations was seen in the presence of a constant in-plane magnetic field, $H_{\parallel ab}$, up to 800 Oe. At such a high in-plane field, the magnetoresistance oscillations showed significant irregularities and instability (Fig. 2d).

To understand the data presented above, the magnetoresistance oscillation signature of the half-flux-quantum states in our samples needs to be analyzed. For simplicity, our sample is modeled as a thin-wall hollow cylinder without leads (Fig. 3a). Starting with a two-component order parameter, the Gibbs free energy per unit length of a cylinder with a wall thickness of w and a radius of r in the thin-wall limit ($w \ll r, \lambda$) as a function

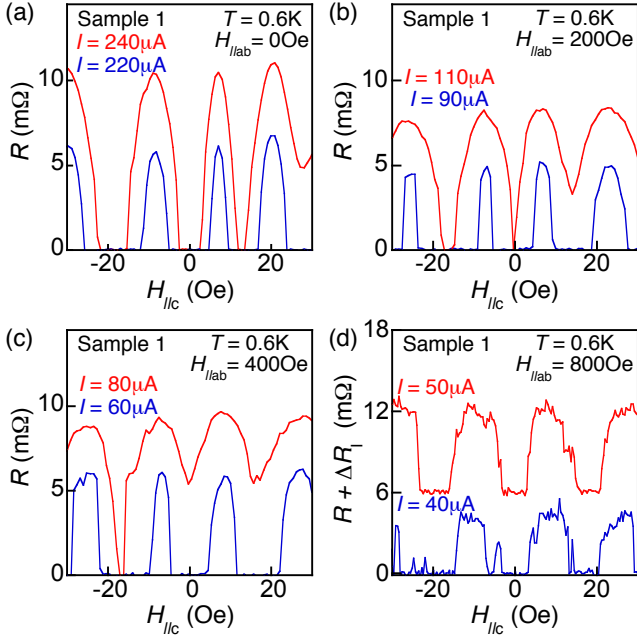


FIG. 2: Magnetoresistance oscillations, R vs. $H_{\parallel c}$, for Sample 1 measured at $T=0.6$ K far below zero-field T_c for an in-plane field of 0 (a), 200 (b), 400 (c) and 800 G (d), respectively. The measurement currents are as indicated. The top curve in (d) is shifted vertically by 6 mΩ for clarity.

of an external field, $H_{\parallel c}$, has the following form, [12, 22]

$$G(n_s, n_{sp}) = \left(\frac{\Phi_0^2}{8\pi^2 r^2} \right) \left(\frac{\beta}{1+\beta} \left[\left(n_s - \frac{\Phi}{\Phi_0} \right)^2 + n_{sp}^2 (1+\beta) \frac{\rho_{sp}}{\rho_s} \right] - \left(\frac{\Phi}{\Phi_0} \right)^2 \right) \quad (1)$$

where $\beta = rw/2\lambda^2$ is the screening parameter, $\Phi = \pi r^2 H_{\parallel c}$ is the applied flux through the cylinder, n_s and n_{sp} are the winding numbers for orbital and spin parts of the order parameter, ρ_s and ρ_{sp} are charge and spin supercurrent densities. A half-flux-quantum state is in general energetically less favorable than a full-flux-quantum state due to the presence of unscreened spin supercurrent, indicated by the n_{sp} term in equation (1). The stability condition for half-flux-quantum states is given as $(1+\beta)(\rho_{sp}/\rho_s) < 1$, which makes the total kinetic energy of the spin and charge currents in the half-flux-quantum state, $\Delta G(l_s = \pm 1/2, l_{sp} = 1/2)$, lower than that of the full-flux-quantum state in the vicinity of $\Phi = \Phi_0/2$, $\Delta G(0, 0)$ or $\Delta G(\pm 1, 0)$. The sample size needs to be sufficiently small, that means a small β , for a given ρ_{sp}/ρ_s in order to reduce the energy cost of the spin supercurrent. The magnetization curves, $\Delta\mu_z$, can be obtained by taking the derivative of the free energy with respect to the applied magnetic field, with the linear background subtracted. It should be noted that the above analysis

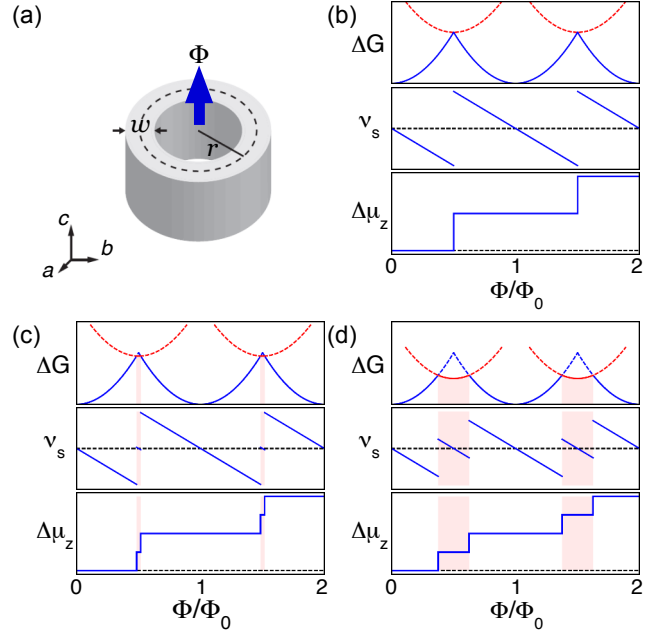


FIG. 3: Superfluid velocity v_s , variation of magnetization $\Delta\mu_z$, and the kinetic part of the Gibbs free energy, ΔG , as a function of Φ calculated from equation (1) for a doubly connected cylinder with $r = 0.58 \mu\text{m}$ and $w = 0.26 \mu\text{m}$, as shown in (a), at a temperature close to T_c (b) and 0.6 K (c); Near T_c , we assume $\rho_{sp}/\rho_s \rightarrow 1$ and $\lambda \rightarrow \infty$; Values of $\rho_{sp}/\rho_s = 0.25$ and $\lambda \sim 166$ nm are used for $T=0.6$ K. Values of ΔG for the full- and half-flux-quantum states are plotted in blue and red, respectively. The light red shadings present the stability regions of the half-flux-quantum state; (d) When the width of the stability region is $\Phi_0/4$, the energy difference between the full- and the half-flux-quantum states at $\Phi = \Phi_0/2$ is 0.31, and the depth of the free energy dip is only 0.04. The scale for ΔG is $0.4(\Phi_0^2/8\pi^2 r^2)\beta/(1+\beta)$.

includes the contribution from neither the spin-orbit coupling, g_{so} nor the superconducting electrical leads. The latter contributes to the Gibbs free energy through the absence of the screening of the spin supercurrent and the spin-orbital coupling.

The value of ρ_{sp}/ρ_s is not known for Sr_2RuO_4 . Numerical studies on the stability regions of half-flux-quantum states based on the torque magnetometry data suggested a value of $\rho_{sp}/\rho_s = 0.25$ at 0.6 K.[17] The ground state free energy shown in Fig. 3 is calculated using parameters of bulk Sr_2RuO_4 . Using the AH model to fit our data we obtain a large penetration depth, and therefore a β value much smaller than expected from that using parameters of the bulk, which favors the presence of the half-flux-quantum state; however, a large value of the penetration depth also suggests a suppression of superconductivity which indicates that ρ_{sp}/ρ_s is likely to be much larger than that used in the numerical study, close to 1. The free energy contribution from in-plane field is given as $\Delta F = -g\mu_B(\rho_\uparrow - \rho_\downarrow)|B_{\parallel ab}|$. [17] Assuming

that $\rho_{\uparrow,\downarrow}$ is independent of Φ , the free energy lowering of the half-flux-quantum state is proportional to the magnitude of the in-plane field. Fig. 3d is obtained by directly shifting the free-energy curve of half-flux-quantum state vertically to match the width of the stability region observed in the torque magnetometry measurements[11]. The free energy variation in the half-flux-quantum state is tiny compared to the free energy difference between the full- and half-flux-quantum states. The sample resistance tracks the free-energy monotonically even though the precise form that is associated with vortex crossing is not known.

With the emergence of the half-flux-quantum state we expect the resistance peaks of Φ_0 oscillations to develop a dip around applied half-flux quanta, especially as the stability regime becomes substantial. For a sample used in our experiment, vortex trapping and pinning within the sample, the free energy contribution from the electrical leads, and the spatial variation of the superconducting order parameter will all complicate the free-energy barrier for the vortex crossing, making sample resistance as a function of the magnetic flux difficult to track. In the torque magnetometry experiment, the entry of parallel vortices was found to be accompanied by the field shift of the transitions between the adjacent fluxoid states and a reduction in the stability region of the half-flux quantum states. In our experiment, the resistance peaks seen in high in-plane fields (Fig. 2d) appear to be flatter than those seen in the smaller in-plane fields (Fig. 2a-c), consistent with theoretical expectations. However, no sharp enough feature tied uniquely to the existence of the half-flux-quantum state was found. Irregularities in magnetoresistance due to random vortex motion make the observation more difficult.

The stability condition described above suggests that thinning the cylinder wall, which is limited by FIB damage that could make the sample nonsuperconducting, favors the emergence of the half-flux-quantum state. We observed unexpected features in Sample 3 with a mean radius $r \approx 545$ nm, mean wall thickness $w \approx 244$ nm and out-of-plane thickness $t \approx 482$ nm (Fig. 4a). The resistance oscillations are smooth and show little hysteresis even under a substantial in-plane field. The sample resistance was found to rise gradually only at one side of the resistance peaks, with a nearly vertical resistance rise on the other side when the measurement current was relatively small (Fig. 4b-4d). A gradual resistance rise started to appear on the other side when the measurement current was further increased to a critical value, suggesting the critical currents of the two arms of the cylinder are different. The critical value was found to be around $60 \mu\text{A}$ for $H_{\parallel ab}=400$ Oe. We estimate that the difference in the critical currents of two arms of the cylinder is on the order of $10 \mu\text{A}$. The measured oscillation period is about 23.7 Oe, which corresponds to an effective radius of 527 nm based on $\Delta H = \Phi_0/(\pi r^2)$, smaller than

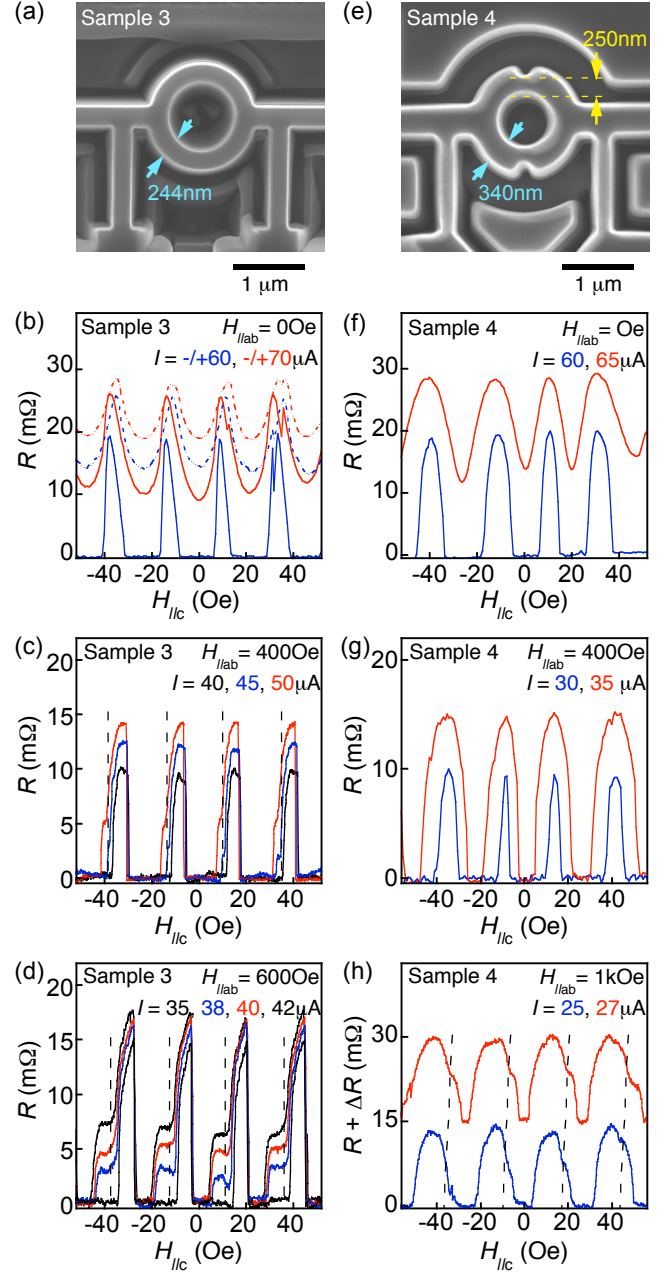


FIG. 4: (a) A SEM image for a Sr_2RuO_4 cylinder, Sample 3. Magnetoresistance oscillation measurement, R vs. $H_{\parallel c}$, with an in-plane field of (b) 0 Oe at $T = 0.6$ K, and (c) 400 Oe and (d) 600 Oe at $T = 0.3$ K for the sample in (a). The measurement currents are indicated starting from the bottom to the top curves. The dash and solid curves in (b) indicate results for positive and negative measurement currents, respectively. (e) A SEM image for a cylinder sample with two constrictions. R vs. $H_{\parallel c}$ measured at $T = 0.3$ K for the sample in (e) with an in-plane field of (f) 0 Oe, (g) 400 Oe and (h) 1000 Oe. The top curve shifted vertically by $15 \text{ m}\Omega$ for clarity in (h).

the value obtained from the SEM image. Dip features in the magnetoresistance oscillations were observed at rela-

tively low in-plane fields, 400 Oe and 600 Oe (Figs. 4c and 4d). Increasing the in-plane field appears to promote the two-peak feature, consistent with the trend for the stability region of the half-flux-quantum state. We speculate that features observed in Sample 3 are the consequence of the half-flux-quantum state even though trapping of vortices in part of the sample may also generate secondary peaks in the magnetoresistance oscillations. In a study of NbSe₂ mesoscopic loops, the field for trapping a vortex in the loop structure was shifted linearly with the measurement current [24] while the field position for the observed resistance peaks in Fig. 4d was found to be insensitive to the measurement current.

The uneven critical currents and the smooth magnetoresistance oscillations found in Sample 3 suggest that this sample may possess a weak link in one arm of the hollow cylinder due to a sample specific reason. Theoretical studies suggest that adding physical constrictions in the superconducting hollow cylinder, the kinetic energy of the spin current relative to that of the charge supercurrent is determined by the narrowest part of the superconducting loop, $\beta = rw_{min}/2\lambda^2$. [23] An additional advantage of the sample with the weak link is that the vortex crossing can be directed to weak link and therefore avoid variation in the free energy barrier along the cylinder circumference, thereby increasing the amplitude of the useful magnetoresistance signals.[24]

In Fig. 4e-4h, results from a sample featuring two constrictions were shown. The sample has a mean radius $r \approx 510$ nm, a wall thickness of 340 nm, and the width of the constriction roughly 250 nm. Since the width of the constrictions in this sample is comparable to the wall thickness of Samples 1 and 2, based on the free-energy consideration, the half-flux-quantum state should appear at a similar in-plane field. Consistently, no feature was seen in the magnetoresistance oscillations at an in-plane field of 400 Oe (Fig. 4g). After an in-plane field of 1000 Oe was applied was a dip found in resistance peaks (Fig. 4h), with features similar to that seen in Sample 3, consistent with expectations from the above analysis.

To conclude, results from the magnetoresistance oscillation measurements suggest that, even though the half-flux-quantum state may indeed exist in micron-sized, doubly connected cylinders of single crystal Sr₂RuO₄, the free energy barely vary as a function of applied flux enclosed in the cylinder within the stability regime. In the torque magnetometry measurements, a plateau in the magnetization can be detected as long as the free energy of the half-flux-quantum state is lower than that of the full-flux-quantum state. The difference of the free energy between them is difficult to determine through the analysis of the measured magnetoresistance oscillations because the connection between the rate of the vortex crossing and the free energy barrier is complicated. Our measurements show that the kinetic energy part of the free energy, which is tuned by the applied magnetic flux,

is only a small part of the total free energy. The spin-orbital coupling to the free energy, which should be large in Sr₂RuO₄, [5] may have made the kinetic part of the free energy even smaller, and the detection of half-flux-quantum through magnetoresistance oscillation measurements significantly more difficult than the torque magnetometry measurements.

We would like to thank H.-Y. Kee, J. Kirtley, Y. Maeno, Z. Wang, Y. Xin, Z. Xu, C.-C. Tsuei, S.-K. Chung, J. K. Jain, C. Kallin, A. J. Leggett, J. A. Sauls, M. Sigrist, V. Varkaruk, K. Roberts, S.-K. Yip, B. Zakrzewski and S. Mills for useful discussions. The work done at Penn State is supported by DOE under Grant No. DE-FG02-04ER46159, at SJTU was supported by MOST of China (2012CB927403). at Tulane by the U.S. Department of Energy under EPSCoR Grant No. de-sc0012432 with additional support from the Louisiana Board of Regents (support for materials synthesis and characterization).

* Electronic address: yxl15@psu.edu

- [1] M. Tinkham, *Introduction to Superconductivity* (McGraw-Hill Book Co., New York, 1996).
- [2] B. S. Deaver and W. M. Fairbank, Phys. Rev. Lett. **7**, 43 (1961).
- [3] R. Doll and M. Nabauer, Phys. Rev. Lett. **7**, 51 (1961).
- [4] W. Little and R. Parks, Phys. Rev. Lett. **9**, 9 (1962).
- [5] H.-Y. Kee, Y. B. Kim, and K. Maki, Phys. Rev. B **64**, R9275 (2000).
- [6] T. M. Rice and M. Sigrist, Journal of Physics: Condensed Matter **7**, L643 (1995).
- [7] G. Baskaran, Physica B **223-224**, 480 (1996).
- [8] A. P. Mackenzie and Y. Maeno, Reviews of Modern Physics **75**, 657 (2003).
- [9] Y. Maeno, S. Kittaka, T. Nomura, S. Yonezawa, and K. Ishida, Journal of the Physical Society of Japan **81**, 011009 (2012).
- [10] Y. Liu and Z.-Q. Mao, Physica C **514**, 339 (2015).
- [11] J. Jang, D. G. Ferguson, V. Vakaryuk, R. Budakian, S. B. Chung, P. M. Goldbart, and Y. Maeno, Science **331**, 186 (2011).
- [12] V. Vakaryuk and A. J. Leggett, Phys. Rev. Lett. **103**, 057003 (2009).
- [13] X. Cai, Y. A. Ying, N. E. Staley, Y. Xin, D. Fobes, T. J. Liu, Z.-Q. Mao, and Y. Liu, Phys. Rev. B **87**, 081104(R) (2013).
- [14] I. Sochnikov, A. Shaulov, Y. Yeshurun, G. Logvenov, and I. Božović, Nature Nanotechnology **5**, 516 (2010).
- [15] V. Vakaryuk and V. Vinokur, Phys. Rev. Lett. **107**, 037003 (2011).
- [16] K. Roberts, Ph.D. dissertation, Chapter 5, University of Illinois at Urbana-Champaign (2015).
- [17] K. Roberts, R. Budakian, and M. Stone, Phys. Rev. B **88**, 094503 (2013).
- [18] P. Santhanam, C. C. Chi, S. J. Wind, M. J. Brady, and J. J. Bucchignano, Phys. Rev. Lett. **66**, 2254 (1991).
- [19] Y. A. Ying, N. E. Staley, Y. Xin, K. Sun, X. Cai, D. Fobes, T. J. Liu, Z.-Q. Mao, and Y. Liu, Nature Communications **4**, 2596 (2013).

- [20] V. O. Dolocan, P. Lejay, D. Mailly, and K. Hasselbach, Phys. Rev. B **74**, 144505 (2006).
- [21] V. O. Dolocan, C. Veauvy, F. Servant, P. L. and K. Hasselbach, Y. Liu, and D. Mailly, Phys. Rev. Lett. **95** (2005).
- [22] S. B. Chung, H. Bluhm, and E.-A. Kim, Phys. Rev. Lett. **99**, 197002 (2007).
- [23] V. Vakaryuk, Ph.D. thesis, University of Illinois at Urbana-Champaign (2010).
- [24] S. A. Mills, C. Shen, Z. Xu, and Y. Liu, Phys. Rev. B **92**, 144502 (2015).